

A New Electroactive and Stable Electrode Based on Praseodymium Molybdate for Symmetrical SOFCs¹

N. V. Lyskov^{a,*}, A. I. Kotova^b, D. I. Petukhov^b, S. Ya. Istomin^b, and G. N. Mazo^b

^a Institute of Problems of Chemical Physics, Russian Academy of Sciences, Chernogolovka, Russia

^b Faculty of Chemistry, Lomonosov Moscow State University, Moscow, Russia

*e-mail: lyskov@icp.ac.ru

Received January 27, 2022; revised April 29, 2022; accepted April 29, 2022

Abstract—The electrochemical activity of a new electrode material based on $\text{Pr}_5\text{Mo}_3\text{O}_{16+\delta}$ (PMO) within the composition of a symmetrical solid oxide fuel cell (S-SOFC) of the electrolyte-supported design is studied. The model S-SOFC of the PMO/Ce_{0.9}Gd_{0.1}O_{1.95}(GDC)/Zr_{0.84}Y_{0.16}O_{1.92}(YSZ)/GDC/PMO composition demonstrated the maximum power density of 28 mW/cm² at 900°C. To improve the power characteristics of S-SOFC, the porous buffer GDC layer is modified by the method of Pr₆O₁₁ infiltration. It is found that the addition of electroactive Pr₆O₁₁ into the GDC buffer layer provides the three-fold increase in the fuel-cell power density with the maximum of 90 mW/cm² at 900°C. The 10 h life-time test of the model S-SOFC with the PMO/GDC + Pr₆O₁₁/YSZ/GDC + Pr₆O₁₁/PMO composition carried out at a load of 0.7 V reveals the absence of any considerable degradation in fuel cell power characteristics. The results obtained suggest that the new electrode material based on PMO holds promise for the development of S-SOFC.

Keywords: praseodymium molybdate, electrode material, electrochemical activity, symmetrical solid-oxide fuel cell

DOI: 10.1134/S102319352211009X

INTRODUCTION

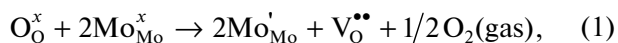
At present, the development of the so-called symmetrical solid oxide fuel cells (S-SOFC) is among the most actively explored directions in the field of electrochemical power sources based on solid oxide fuel cells (SOFC) [1–3]. Their characteristic feature is that both electrodes are made of materials of one and the same chemical composition and are capable of performing both anodic and cathodic electrochemical functions. The transition from traditional SOFCs to symmetrical cells can save energy consumed during their fabrication due to the smaller number of thermal treatment stages involved. Moreover, this can make cells more tolerant with respect to the quality of hydrocarbon fuel because the problem of anode poisoning by sulfur and carbon can be solved by their oxidation by cathodic gases briefly supplied to the anode (depolarization) [1, 4, 5]. When choosing the electrode materials for a S-SOFC one has to bear in mind that this material should exhibit the thermal and phase stability in both oxidative and reductive atmospheres as well as provide the high rate of anodic and cathodic electrochemical reactions. Moreover, its high-temperature conductivity in a wide interval of partial oxy-

gen pressure should not be below 1 S cm⁻¹ and the thermal expansion coefficient (TEC) should be comparable with that of the solid-electrolyte material [3].

The list of materials suitable for electrodes in S-SOFC as regards their physicochemical properties is limited. The literature contains mainly the studies of complex oxides of *d* metals with the perovskite structure or its derivatives [1–3]. The advantages of oxides with the perovskite structure as the SOFC electrode materials are their high conductivity, thermodynamic stability, and catalytic activity in electrode reactions [6–10]. It should be noted that the main drawback of these materials lies in their high chemical activity in reactions with the other SOFC components, particularly, electrolytes based on Zr_{0.84}Y_{0.16}O_{1.92} (YSZ) and Ce_{0.9}Gd_{0.1}O_{1.95} (GDC) [11–16]. This drawback is mainly associated with the presence of coarse and, hence, basic cations such Sr²⁺ and Ba²⁺ in their composition. This is why the quest for electrode materials based on oxides with the other than perovskite structure is important. Only several S-SOFC electrode materials of this kind are known: cermet Ni_{0.7}Co_{0.3}O–Ce_{0.8}Sm_{0.2}O_{1.9} [17], LiNi_{0.8}Co_{0.15}Al_{0.05}O₂ [18], and also Fe_{0.5}Mg_{0.25}Ti_{0.25}Nb_{0.9}Mo_{0.1}O_{4–δ} (FMTMN) with the α-PbO₂ structure [19].

¹ A tribute to outstanding electrochemist Oleg Aleksandrovich Petrii (1937–2021).

From our point of view, the most promising candidates for new electrode materials for S-SOFC are molybdenum-containing oxides which crystallize in the perovskite and fluorite structure types. This is due to the fact that in these phases, the molybdenum cations easily change their degree of oxidation with variation of the partial oxygen pressure but retain their crystal structure. At the same time, the oxygen vacancies in their structure are formed sufficiently easily which makes possible the fast oxygen-ion transport, and the latter favors the increase in the efficiency of the oxygen reduction reaction on the SOFC cathode. Considering the behavior of molybdenum-containing SOFC oxides in the reductive atmosphere, the partial reduction of molybdenum cations ($\text{Mo}^{6+} \rightarrow \text{Mo}^{5+}$) gives rise to the appearance of electrons as the charge carriers. This process can be expressed by the following quasi-chemical equation:



where O_O^\times is the oxygen ion in its regular position, $\text{Mo}_{\text{Mo}}^\times$ is the Mo^{6+} ion in its regular position, Mo'_{Mo} is the Mo^{5+} ion in its regular position, $\text{V}_\text{O}^{\bullet\bullet}$ is the oxygen vacancy. As a result, the transition from *p* to *n* conduction can occur which will favor the higher conductivity of the oxide in the reductive atmosphere of anodic gases in SOFC.

In the recent years, the molybdenum-containing oxides of rare-earth elements (REE) with the fluorite-like structure and the $\text{R}_5\text{Mo}_3\text{O}_{16+\delta}$ composition, where $\text{R} = \text{REE}$, are becoming the potential candidates for SOFC electrode materials [20–23]. Their crystalline structure and certain high-temperature properties were studied earlier [21–24]. The high-temperature studies of the properties of $\text{Pr}_5\text{Mo}_3\text{O}_{16+\delta}$ (PMO) [20, 21] with the aim of using it as the electrode material revealed that both in air and under reductive conditions [21] its TEC is comparable with the TEC of solid electrolytes with the fluorite structure based on YSZ and GDC traditionally used in SOFC. At the same time, PMO exhibits chemical stability with respect to YSZ (up to 950°C) and GDC (up to 1000°C) and its conductivity in the reductive atmosphere is equal to 1.2 S/cm at 800°C [21]. By studying the electrochemical activity of electrode materials based on PMO deposited on the surface of a GDC solid electrolyte, it was shown that the polarization resistance (R_p) of a PMO electrode at 800°C is 8.8 and 4.8 $\Omega \text{ cm}^2$ in air and the reductive atmosphere, respectively [20]. Moreover, R_p can be decreased by one order of magnitude down to 0.6 $\Omega \text{ cm}^2$ by passing from the monophase PMO electrode to the composite PMO– $x\text{Pr}_6\text{O}_{11}$ ($x = 50 \text{ wt } \% \text{ Pr}_6\text{O}_{11}$). However, the possibility of the practical application of this PMO-based electrode material in S-SOFC is still unclear.

This study is devoted to its investigation as the electrode material for S-SOFC.

EXPERIMENTAL

The single phase PMO powder was synthesized by the solid state method in air [20]. As the precursors, the oxides Pr_6O_{11} (Sigma-Aldrich, 99.9%) and MoO_3 (Sigma-Aldrich, 99.97%) were taken in stoichiometric ratios. The praseodymium oxide was preliminarily annealed at 350°C for 10 h in air to remove the traces of carbon dioxide and water sorbed on the surface. The mixture of precursors with the addition of heptane was homogenized in a planetary mill (Fritzch Pulverisette 6, Germany) for 30 min (rotation rate 600 rpm). Then, the powder was dried in air until the complete removal of heptane, pressed to pellets, and subjected to step-wise heating: at 600°C for 30 h and then at 1000°C for 58 h. The phase composition of the synthesized compound was controlled by the X-ray diffraction (XRD) analysis by means of Huber G670 with Image Plate detector ($\text{CuK}_{\alpha 1}$ radiation, 2θ interval 3°–100°, acquisition time 30 min). The XRD data were processed by using the STOE WinXpow (Ver. 1.04) program.

The electrochemical characteristics of PMO as the material for S-SOFC electrodes were studied on a specially prepared model symmetrical fuel cell of the electrolyte-supported design and the PMO/GDC/YSZ/GDC/PMO composition. The cationic composition of the GDC and YSZ solid electrolytes corresponded to that mentioned in the Introduction Section. In the first stage of their preparation, the gas-tight ceramic YSZ membranes 450–500 μm thick and 24 mm in diameter were obtained. As the starting reagent, we used commercial single phase YSZ powder (particle size $0.5 \pm 0.2 \mu\text{m}$, Ningbo SOFCMAN Energy Technology, China) which was sintered at 1400°C for 10 h in air. According to the results of hydrostatic weighing, its relative density was ~95% of its XRD density. After this, a GDC buffer electrolyte layer was formed on the surface of thus obtained YSZ membranes. For this purpose, a suspension of powders of GDC (particle size 0.5–3 μm , Ningbo SOFCMAN Energy Technology, China) and rice starch (particle size 3–5 μm , Deffner & Johann, Germany) was prepared in the ratio of 80 : 20 wt %, respectively, with addition of an organic binder (α -terpineol) [25]. The mass ratio of the powder mixture and α -terpineol was 2 : 1. The suspension was screen printed by using fabric meshes VS-Monoprint PES HT TW 77/55 (Verseidag-Techfab, Germany). The screen-printing procedure on each side of the YSZ membrane was repeated twice. After each printing, the sample was dried at 130°C for 1 h. The thus deposited GDC layer was sintered at 1300°C for 6 h in air. In addition, we prepared samples with the GDC buffer layer modified by adding a portion of electrocatalytically active Pr_6O_{11} . The procedure of infiltrating praseodymium(III) nitrate and its further thermal treat-

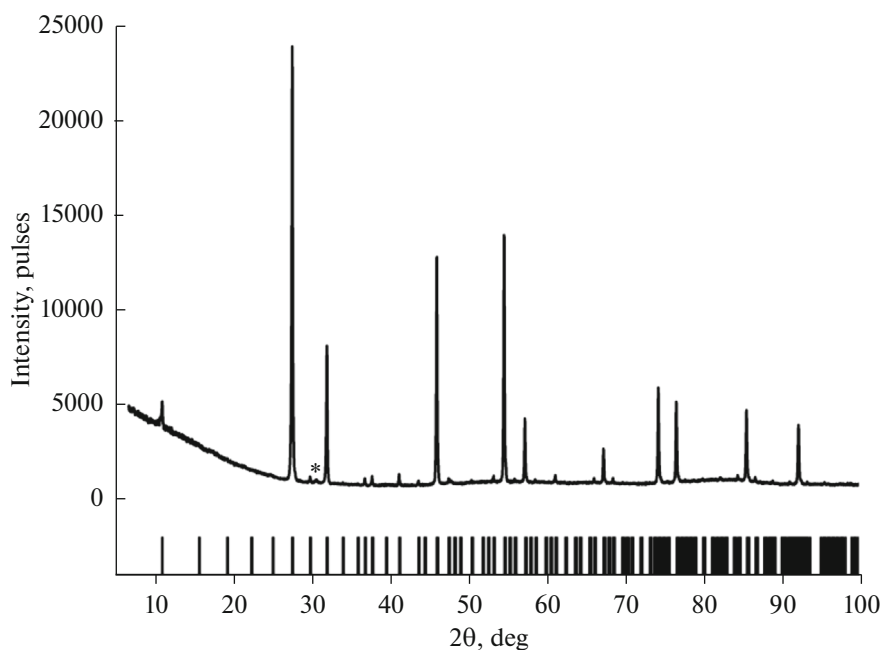


Fig. 1. X-ray diffraction pattern of the synthesized $\text{Pr}_5\text{Mo}_3\text{O}_{16+\delta}$ powder (vertical bars on the bottom show the calculated positions of the PMO phase reflections, the asterisk marks the position of the unidentified admixture phase reflection).

ment is described in detail in [25]. The amount of Pr_6O_{11} added to the porous GDC buffer layer was about 30 wt % with respect to the porous layer mass. The PMO electrode layer was deposited after the formation of the GDC buffer layer in the final stage of fabrication of symmetrical fuel cells. For this purpose, we prepared the electrode paste of the synthesized PMO powder and an organic binder (Heraeus V006, Germany) in the mass ratio 1 : 1 and screen printed it by the similar procedure as that described above. The procedure of deposition of the electrode material was repeated twice. After this, the samples were dried at 130°C for 1 h and annealed at 900°C for 4 h in air. The electrode surface was 2 cm^2 .

To analyze the microstructure of samples, we used the technique of scanning electron microscopy (SEM). To study the cross fractures of samples, we used electron microscope LEO Supra 50VP (Germany). The cationic composition of the electrode/electrolyte interface was studied on electron microscope TM4000Plus (Hitachi, Japan) by the energy-dispersive X-ray spectroscopy (EDX). For this purpose, a multichannel energy-dispersive X-ray spectrometer INCA Energy 350X-Max 80 (Oxford Instruments, UK) was used. The porosity and the thickness of electrode layers were assessed by analyzing the cross fractures of samples by using the Image J software.

The electrochemical tests of model S-SOFCs were carried out in a ceramic measuring cell ProbostatTM (NorECs AS, Norway) in the temperature range of $800\text{--}900^\circ\text{C}$. Platinum wires were used as the current

leads, the current-collecting contacts were made of platinum nets closely pressed to electrodes. The sample temperature was measured by means of the Pt–Pt/Rh thermocouple placed near the sample. As the fuel, we used the wet (3 vol % H_2O) argon–hydrogen mixture (50 : 50 vol %) and also the argon–oxygen mixture as the oxidizer (80 : 20 vol %). The rate of reagent delivery was controlled by Bronkhorst (Netherlands) mass flow controllers at a level of 90 mL/min. The voltammetric characteristics (VAC) were measured by means of an Autolab PGSTAT302N potentiostat-galvanostat equipped with a module for measuring impedance FRA 32M (Netherlands) in the potential scanning mode in the range from 1000 to 100 mV at the scanning rate of 20 mV/s. The impedance studies of the fuel cells and also of the control samples of YSZ electrolyte with deposited platinum electrodes were carried out at open circuit voltage in the frequency range from 0.1 to 10^6 Hz with the signal amplitude of 10 mV in the temperature range of $800\text{--}900^\circ\text{C}$.

RESULTS AND DISCUSSION

Figure 1 shows an X-ray diffraction pattern of the PMO sample synthesized by the solid state method in air. According to XRD data, the PMO sample is virtually single phase (the maximum intensity of the unidentified admixture phase reflection $\ll 1\%$). The reflections corresponding to the PMO phase were identified in cubic syngony as the space group $Pn\text{-}3n$ with the unit cell parameter $a = 11.0968(1)\text{ \AA}$, in

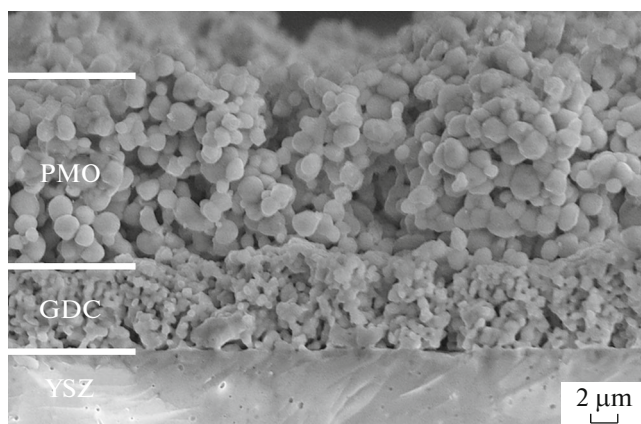


Fig. 2. SEM image of the cross section of the PMO electrode/GDC buffer layer/YSZ electrolyte interface in the model S-SOFC of the PMO/GDC/YSZ/GDC/PMO composition.

agreement with the literature data: $a = 11.1007(3) \text{ \AA}$ [24] and $a = 11.0897(1) \text{ \AA}$ [26]. The scatter of unit cell parameter was apparently associated with the different content of oxygen in $\text{Pr}_5\text{Mo}_3\text{O}_{16+\delta}$ samples obtained under different experimental conditions.

The microstructure of the electrode material and the way of organization of the electrode/electrolyte boundary are among the key factors determining the efficiency of a SOFC. The porous electrode structure and the accessibility of reagents to reaction sites on the electrode/electrolyte interface favor the high rate of electrochemical reactions.

Figure 2 shows the SEM image of the interface: PMO electrode/GDC buffer layer/YSZ electrolyte of the model S-SOFC with the PMO/GDC/YSZ/GDC/PMO composition. The electrode and buffer layers had the well-developed surface and were characterized by the uniform size distribution of particles and pores. Moreover, the pores formed a connected net of channels which provided good access for gas throughout the whole layer. The good adhesion between the GDC buffer layer and the surface of the YSZ solid-electrolyte membrane and also between the PMO electrode layer and the GDC buffer layer deserves mention. The thickness of the PMO electrolyte layer was $\sim 20 \mu\text{m}$ and the thickness of the GDC buffer layer was $\sim 8 \mu\text{m}$.

Figure 3 summarizes the data on voltammetric and power characteristics of the model S-SOFC with the PMO/GDC/YSZ/GDC/PMO composition as a function of the working temperature. As the temperature increased from 800 to 900°C, the maximum power density of the symmetrical fuel cell increased from 13 to 28 mW/cm^2 .

To assess the ohmic and polarization contributions to the overall resistance of the fuel cell, the latter was studied by impedance spectroscopy in the open circuit voltage mode. Figure 4 shows the impedance spectra of the S-SOFC with PMO/GDC/YSZ/GDC/PMO composition measured as the working temperature varied from 800 to 900°C. The ohmic resistance (R_{ohm}) of the sample was found by approximating the impedance spectrum to the real axis in the high-frequency limit. This value is preferentially determined by the resis-

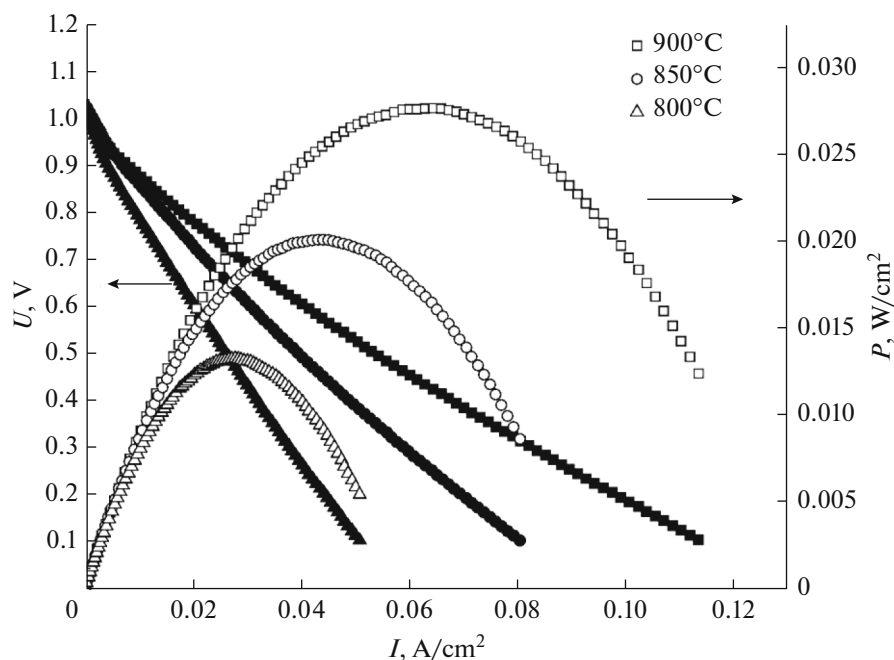


Fig. 3. Voltammetric (closed symbols) and power density (open symbols) characteristics of the model S-SOFC with the PMO/GDC/YSZ/GDC/PMO composition as a function of its working temperature (temperature measurement error $\pm 3^\circ\text{C}$).

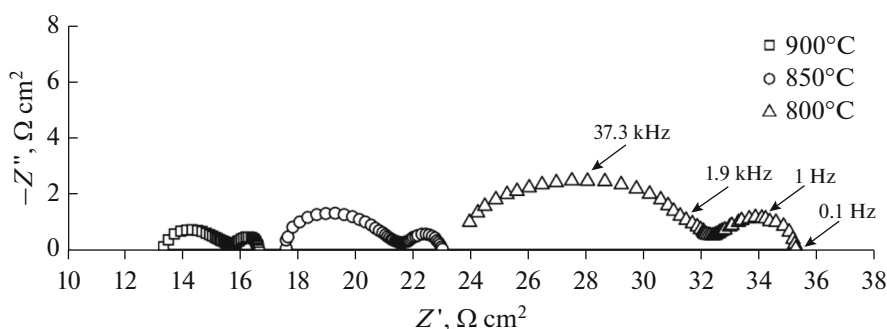


Fig. 4. Impedance spectra of the S-SOFC with the PMO/GDC/YSZ/GDC/PMO composition measured in the open circuit voltage mode as a function of its working temperature (temperature measurement error $\pm 3^\circ\text{C}$).

tance of the solid electrolyte material. The overall polarization loss on electrodes (R_η) was calculated based on the difference between low and high-frequency cutoffs on the real axis of the impedance spectrum. Table 1 shows the calculated R_{ohm} and R_η values normalized to the electrode surface. It is evident that the main contribution to the power loss of the fuel cell is preferentially made by the ohmic resistance.

Recently, to increase the specific power characteristics of a SOFC, in addition to the methods of decreasing the ohmic resistance by decreasing the thickness of the electrolyte layer and the transition to the electrode-supported design, it was proposed to increase the electrochemical activity of the electrode by infiltrating electroactive Pr_6O_{11} additive into the preliminarily developed porous structure. To form the latter, the materials of solid electrolyte or cathode can be used [25, 27–29]. The choice of praseodymium oxide is associated with its high efficiency in redox reactions. Moreover, the absence of interaction between Pr_6O_{11} and the solid electrolyte of YSZ [30] and GDC [25] at temperature above 1000°C is also important. In connection with this, we prepared a modified S-SOFC in which an electrocatalytically active addition of Pr_6O_{11} was carried out by its infiltration into the porous GDC buffer layer (PMO/GDC + Pr_6O_{11} /YSZ/GDC + Pr_6O_{11} /PMO).

Figures 5 and 6a show the SEM images of the interface: PMO/GDC buffer layer modified with Pr_6O_{11} /YSZ electrolyte. In this case, the GDC sub-layer has also the well-developed surface. The EDX results (Figs. 6b, 6c) showed that the electroactive Pr_6O_{11} phase covers the inner volume of pores in the GDC layer; and, moreover, submicron Pr_6O_{11} particles form a connected structure on the GDC surface, which should provide the formation of new electroactive sites involved in redox reactions.

Figure 7 shows the voltammetric and power characteristics of the model S-SOFC of the PMO/GDC + Pr_6O_{11} /YSZ/GDC + Pr_6O_{11} /PMO composition as a function of the working temperature. The maximum power density of the fuel cell increased from 30 to

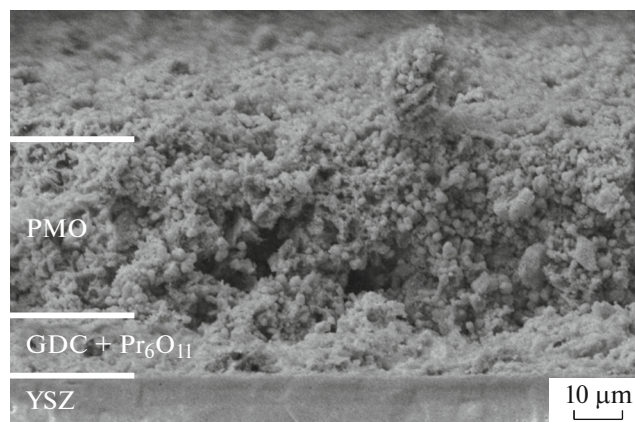


Fig. 5. SEM image of the cross section of the interface (PMO electrode/GDC buffer layer modified infiltrated Pr_6O_{11} /YSZ electrolyte) in the model S-SOFC with PMO/GDC + Pr_6O_{11} /YSZ/GDC + Pr_6O_{11} /PMO composition.

90 mW/cm^2 as the temperature increased from 700 to 900°C . A comparison of power characteristics of the model S-SOFCs showed that the addition of electroactive Pr_6O_{11} into the GDC buffer layer provided the three-fold increase in the maximum power density of the fuel cell.

The impedance studies of the model S-SOFC with the PMO/GDC + Pr_6O_{11} /YSZ/GDC + Pr_6O_{11} /PMO composition (Fig. 8) showed that the electroactive

Table 1. Calculated values of ohmic (R_{ohm}) and polarization (R_η) resistance of the S-SOFC with the PMO/GDC/YSZ/GDC/PMO composition upon varying the working temperature from 800 to 900°C

$T, ^\circ\text{C}$	$R_{\text{ohm}}, \Omega \text{ cm}^2$	$R_\eta, \Omega \text{ cm}^2$
900	13.3	3.4
850	17.6	5.4
800	23.4	11.9

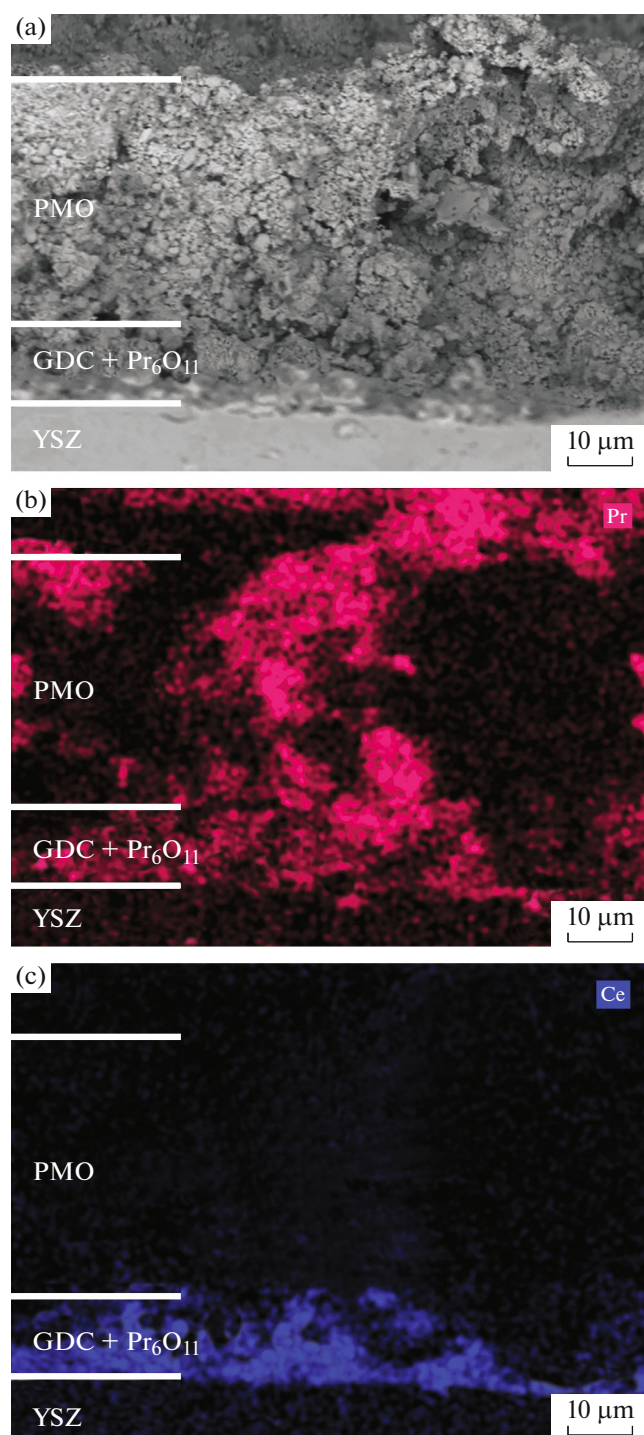


Fig. 6. (a) SEM image of the cross section of the interface (PMO electrode/GDC buffer layer modified by infiltrated Pr_6O_{11} /YSZ electrolyte for a model S-SOFC of the PMO/GDC + Pr_6O_{11} /YSZ/GDC + Pr_6O_{11} /PMO composition); (b) distribution map of (red areas) praseodymium over the surface of the electrode/electrolyte interface cross section; (c) distribution map (blue regions) of cerium over the surface of the electrode/electrolyte interface cross section.

Pr_6O_{11} additive favored not only the lower polarization losses on the electrode, but also the lower ohmic losses. Table 2 shows the calculated values of R_{ohm} and R_{η} for the model S-SOFC with the PMO/GDC + Pr_6O_{11} /YSZ/GDC + Pr_6O_{11} /PMO composition. To understand the reasons for so considerable decrease in ohmic losses, let us compare the specific ionic conductivity of the YSZ solid electrolyte determined from the impedance data for the symmetrical Pt/YSZ/Pt cell (Fig. 9) with the conductivity calculated based on R_{ohm} in the experiments on studying the power characteristics of fuel cells PMO/GDC/YSZ/GDC/PMO (cell 1) and PMO/GDC + Pr_6O_{11} /YSZ/GDC + Pr_6O_{11} /PMO (cell 2). For cell 2, where the diffusion paths of oxygen ions are in fact limited by the thickness of the YSZ layer (because the GDC buffer layers covered by the electrocatalyst layer play the role of electrodes), the conductivity calculated from the R_{ohm} value is comparable with the specific conductivity of the YSZ solid electrolyte layer. In contrast, for cell 1, in which the electrolyte membrane represents a combination of layers GDC/YSZ/GDC, the conductivity is lower by a factor of ~ 6 as compared with the conductivity of solid-electrolyte membrane in cell 2. Apparently, in this case the key role is played not by the ohmic resistance of YSZ, but by the combined contribution of the resistance of the porous GDC buffer layer and the resistance of the GDC/YSZ interface, which increase the diffusion paths of oxygen ions and favor the higher ohmic resistance for the fuel cell PMO/GDC/YSZ/GDC/PMO. Despite the increase in the specific power characteristics and the decrease its total resistance including ohmic and polarization contributions, the ratio between R_{ohm} and R_{η} remains at a level of 3 : 1. Based on this, we can conclude that as in the previous case, the ohmic resistance makes the main contribution to the power losses of the fuel cell. Thus, the subsequent modernization of S-SOFC with the use of PMO as the electrode material may be associated with the transition from the electrolyte-supported to electrode-supported design.

To check the time stability of electrochemical characteristics of the S-SOFC with the PMO/GDC + Pr_6O_{11} /YSZ/GDC + Pr_6O_{11} /PMO composition, we carried out its life-time tests at the temperature of

Table 2. Calculated values of ohmic (R_{ohm}) and polarization (R_{η}) resistances of the S-SOFC with the PMO/GDC + Pr_6O_{11} /YSZ/GDC + Pr_6O_{11} /PMO composition as a function of the working temperature in the interval from 800 to 900°C

$T, ^\circ\text{C}$	$R_{\text{ohm}}, \Omega \text{ cm}^2$	$R_{\eta}, \Omega \text{ cm}^2$
900	2.17	0.67
850	2.33	0.89
800	3.19	1.19

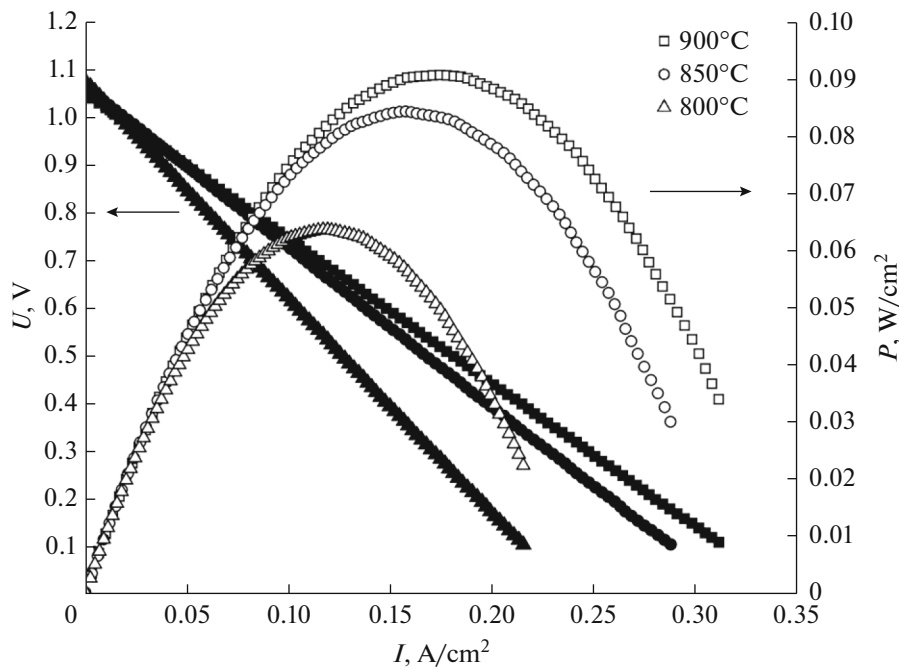


Fig. 7. Voltammetric (closed symbols) and power density (open symbols) characteristics of the model S-SOFC with the PMO/GDC + Pr₆O₁₁/YSZ/GDC + Pr₆O₁₁/PMO composition as a function of its working temperature (temperature measurement error ±3°C).

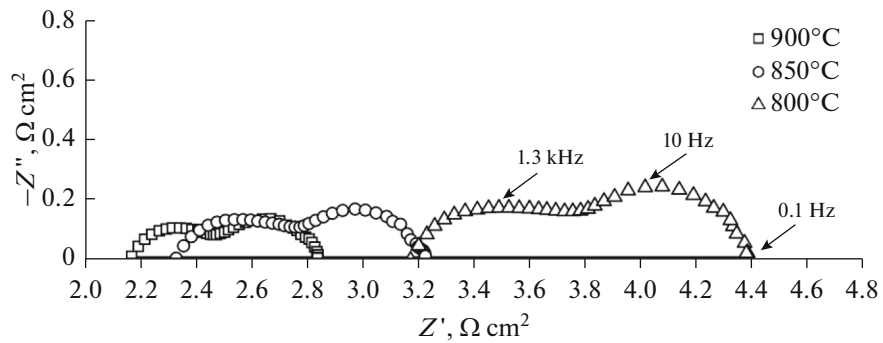


Fig. 8. Impedance spectra of the S-SOFC with the PMO/GDC + Pr₆O₁₁/YSZ/GDC + Pr₆O₁₁/PMO composition measured in the open circuit voltage mode (temperature measurement error ±3°C).

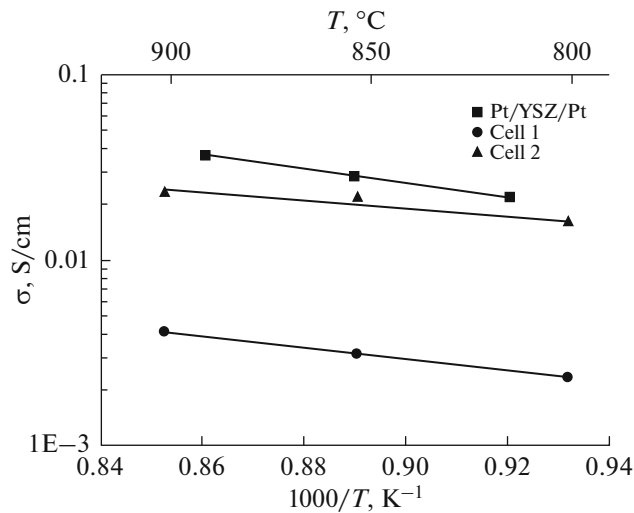


Fig. 9. A comparison of the conductivity of the YSZ solid electrolyte with its value calculated based on R_{ohm} for the fuel cells (cell 1) PMO/GDC/YSZ/GDC/PMO and (cell 2) PMO/GDC + Pr₆O₁₁/YSZ/GDC + Pr₆O₁₁/PMO.

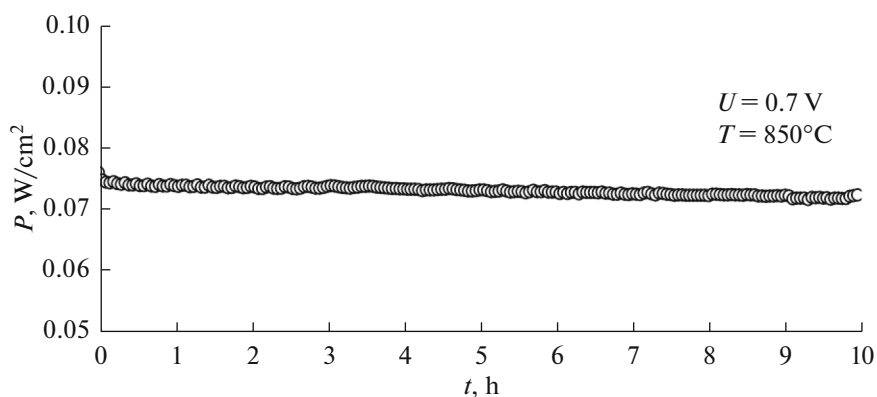


Fig. 10. The time dependence of the power density of the model S-SOFC with the PMO/GDC + Pr₆O₁₁/YSZ/GDC + Pr₆O₁₁/PMO at the potential of 0.7 V and 850°C.

850°C for 10 h under the conditions of its operation under load in the potentiostatic mode at the potential of 0.7 V. Figure 10 shows the dependence of the fuel-cell power density in time. No sharp decrease in the power characteristics of the fuel cell under load was observed during the experiment. The power density of the loaded fuel cell at the potential of 0.7 V during its 10 h continuous operation decreased by ~2.7%.

CONCLUSIONS

Studying the electrochemical characteristics of a model S-SOFC of the electrolyte-supported design PMO/GDC/YSZ/GDC/PMO with the new electrode material based on praseodymium molybdate PMO crystallized in the fluorite-like structure has shown that the maximum power density of 28 mW/cm² is reached at 900°C. Modifying the porous GDC buffer layer by infiltrating Pr₆O₁₁ allowed the maximum power density to be increased to 90 mW/cm² at 900°C. The 10 h life-time tests of the S-SOFC sample with the PMO/GDC + Pr₆O₁₁/YSZ/GDC + Pr₆O₁₁/PMO composition at the potential of 0.7 V revealed the absence of any substantial degradation of power characteristics for a fuel cell under load. Thus, these results suggest that the proposed PMO-based electrode material and the approaches aimed at the development of S-SOFC with electrode materials of the structure different from perovskites hold promise. Most probably, the further improvement of power characteristic can be achieved by the transition to the PMO–Pr₆O₁₁ composite electrodes.

ACKNOWLEDGMENTS

S.Ya. Istomin is grateful to the Interdisciplinary Scientific and Educational School of the Lomonosov Moscow State University: “The Future of the Planet and Global Environmental Changes” for supporting his investigations.

FUNDING

This study supported by the Russian Foundation for Basic Research (grant no. 20-08-00454). The materials used were synthesized within the framework of the State Task for the Institute of Problems of Chemical Physics (no. AAAA-A19-119061890019-5).

CONFLICT OF INTEREST

The authors declare that they have no conflict of interest.

REFERENCES

- Istomin, S.Ya., Lyskov, N.V., Mazo, G.N., and Antipov, E.V., Electrode materials based on complex *d*-metal oxides for symmetrical solid oxide fuel cells, *Russ. Chem. Rev.*, 2021, vol. 90, p. 644.
- Su, C., Wang, W., Liu, M., Tadé, M.O., and Shao, Z., Progress and prospects in symmetrical solid oxide fuel cells with two identical electrodes, *Adv. Energy Mater.*, 2015, vol. 5, p. 1500188.
- Ruiz-Morales, J.C., Marrero-López, D., Canales-Vázquez, J., and Irvine, J.T., Symmetric and reversible solid oxide fuel cells, *RSC Adv.*, 2011, vol. 1, p. 1403.
- Cowin, P.I., Petit, C.T., Lan, R., Irvine, J.T., and Tao, S., Recent progress in the development of anode materials for solid oxide fuel cells, *Adv. Energy Mater.*, 2011, vol. 1, p. 14.
- Ge, X.M., Chan, S.H., Liu, Q.L., and Sun, Q., Solid oxide fuel cell anode materials for direct hydrocarbon utilization, *Adv. Energy Mater.*, 2012, vol. 2, p. 1156.
- Ishihara, T., *Perovskite oxide for solid oxide fuel cells*. New York: Springer Science & Business, 2009. 302 p.
- Tilley, R.J.D., *Perovskites: structure – property relationships*. Chichester: Wiley, 2016. 327 p.
- Sadykov, V.A., Muzykantov, V.S., Yermeev, N.F., Pelipenko, V.V., Sadovskaya, E.M., Bobin, A.S., Fedorova, Yu.E., Amanbaeva, D.G., and Smirnova, A.L., Solid oxide fuel cell cathodes: importance of chemical composition and morphology, *Catal. Sustain. Energy*, 2015, vol. 2, p. 57.

9. Shu, L., Sunarso, J., Hashim, S.S., Mao, J., Zhou, W., and Liang, F., Advanced perovskite anodes for solid oxide fuel cells: A review, *Int. J. Hydrogen Energy*, 2019, vol. 44, p. 31275.
10. Istomin, S.Ya. and Antipov, E.V., Cathode materials based on perovskite-like transition metal oxides for intermediate temperature solid oxide fuel cells, *Russ. Chem. Rev.*, 2013, vol. 82, p. 686.
11. Kostogloudis, G.Ch., Tsiniarakis, G., and Ftikos, Ch., Chemical reactivity of perovskite oxide SOFC cathodes and yttria stabilized zirconia, *Solid State Ionics*, 2000, vol. 135, p. 529.
12. Zhang, L., Chen, G., Dai, R., Lv, X., Yang, D., and Geng, Sh., A review of the chemical compatibility between oxide electrodes and electrolytes in solid oxide fuel cells, *J. Power Sources*, 2021, vol. 492, p. 229630.
13. Van Roosmalen, J.A.M. and Cordfunke, E.H.P., Chemical reactivity and interdiffusion of (La,Sr)MnO₃ and (Zr,Y)O₂ solid oxide fuel cell cathode and electrolyte materials, *Solid State Ionics*, 1992, vol. 52, p. 303.
14. Yokokawa, H., H. Sakai, H., Kawada, T., and Dokiya, M., Thermodynamic analysis of reaction profiles between LaMO₃ (M = Ni, Co, Mn) and ZrO₂, *Solid State Ionics*, 1991, vol. 138, p. 2719.
15. Dos Santos-Gomez, L., Leon-Reina, L., Porrás-Vázquez, J.M., Losilla, E.R., and Marrero-Lopez, D., Chemical stability and compatibility of double perovskite anode materials for SOFC, *Solid State Ionics*, 2013, vol. 239, p. 1.
16. Marrero-Lopez, D., Pena-Martínez, J., Ruiz-Morales, J.C., Gabas, M. P., Nunez, M.A. Aranda, G., and Ramos-Barrado, J.R., Redox behaviour, chemical compatibility and electrochemical performance of Sr₂MgMoO_{6-δ} as SOFC anode, *Solid State Ionics*, 2010, vol. 180, p. 1672.
17. Chen, Y., Cheng, Z., Yang, Y., Yu, W., Tian, D., Lu, X., Ding, Y., and Lin, B., Improved performance of symmetrical solid oxide fuel cells with redox-reversible cermet electrodes, *Mater. Lett.*, 2017, vol. 188, p. 413.
18. Chen, G., Sun, W., Luo, Y., Liu, H., Geng, S., Yu, K., and Liu, G., Investigation of layered Ni_{0.8}Co_{0.15}Al_{0.05}LiO₂ in electrode for low-temperature solid oxide fuel cells, *Int. J. Hydrogen Energy*, 2018, vol. 43, p. 417.
19. Ni, C., Feng, J., Cui, J., Zhou, J., and Ni, J., An n-type oxide Fe_{0.5}Mg_{0.25}Ti_{0.25}Nb_{0.9}Mo_{0.1}O_{4-δ} for both cathode and anode of a solid oxide fuel cell, *J. Electrochem. Soc.*, 2017, vol. 164, p. F283.
20. Lyskov, N.V., Kotova, A.I., Istomin, S.Ya., Mazo, G.N., and Antipov, E.V., Electrochemical properties of electrode materials based on Pr₅Mo₃O_{16+δ}, *Russ. J. Electrochem.*, 2020, vol. 56, p. 93.
21. Istomin, S.Ya., Kotova, A.I., Lyskov, N.V., Mazo, G.N., and Antipov, E.V., Pr₅Mo₃O_{16+δ}: A new anode material for solid oxide fuel cells, *Russ. J. Inorg. Chem.*, 2018, vol. 63, p. 1291.
22. Antipin, A.M., Alekseeva, O.A., Sorokina, N.I., Kusikova, A.N., Artemov, V.V., Murzin, V.Y., Kharitonova, E.P., Orlova, E.A., and Voronkova, V.I., Structure of compound Pr₅Mo₃O_{16+δ} exhibiting mixed electronic-ionic conductivity, *Crystallogr. Rep.*, 2015, vol. 60, p. 640.
23. Voronkova, V.I., Leonidov, I.A., Kharitonova, E.P., Belov, D.A., Patrakeev, M.V., Leonidova, O.N., and Kozychevnikov, V.L., Oxygen ion and electron conductivity in fluorite-like molybdates Nd₅Mo₃O₁₆ and Pr₅Mo₃O₁₆, *J. Alloys Compd.*, 2014, vol. 615, p. 395.
24. Tsai, M., Greenblatt, M., and McCarroll, W.H., Oxide ion conductivity in Ln₅Mo₃O_{16+x} (Ln = La, Pr, Nd, Sm, Gd; x = 0.5), *Chem. Mater.*, 1989, vol. 1, p. 253.
25. Lyskov, N.V., Galin, M.Z., Napol'skii, K.S., Roslyakov, I.V., and Mazo, G.N., Increasing the electrochemical activity of the interface Pr_{1.95}La_{0.05}CuO₄/porous Ce_{0.9}Gd_{0.1}O_{1.95} layer by infiltrating Pr₆O₁₁, *Russ. J. Electrochem.*, 2021, vol. 57, p. 670.
26. Martínez-Lope, M.J., Alonso, J.A., Sheptyakov, D., and Pomyakushin, V., Preparation and structural study from neutron diffraction data of Pr₅Mo₃O₁₆, *J. Solid State Chem.*, 2010, vol. 183, p. 2974.
27. Ding, D., Li, X., Lai, S.Y., Gerdes, K., and Liu, M., Enhancing SOFC cathode performance by surface modification through infiltration, *Energy Environ. Sci.*, 2014, vol. 7, p. 552.
28. Nicollet, C., Flura, A., Vibhu, V., Rougier, A., Basat, J.M., and Grenier, J.C., An innovative efficient oxygen electrode for SOFC: Pr₆O₁₁ infiltrated into Gd-doped ceria backbone, *Int. J. Hydrogen Energy*, 2016, vol. 41, p. 15538.
29. Connor, P.A., Yue, X., Savaniu, C.D., Price, R., Triantafyllou, G., Cassidy, M., Kerherve, G., Payne, D.J., Maher, R.C., Cohen, L.F., Tomov, R.I., Glowacki, B.A., Kumar, R.V., and Irvine, J.T.S., Tailoring SOFC electrode microstructures for improved performance, *Adv. Energy Mater.*, 2018, vol. 8, p. 1800120.
30. Taguchi, H., Chiba, R., Komatsu, T., Orui, H., Watanabe, K., and Hayashi, K., LNF SOFC cathodes with active layer using Pr₆O₁₁ or Pr-doped CeO₂, *J. Power Sources*, 2013, vol. 241, p. 768.

Translated by T. Safonova